Pre- and Postsynaptic Properties Regulate Synaptic Competition through Spike-Timing-Dependent Plasticity

Hana Ito and Katsunori Kitano

Department of Human and Computer Intelligence, Ritsumeikan University,
1-1-1 Nojihigashi, Kusatsu, Shiga 5258577, Japan
hana@cns.ci.ritsumei.ac.jp, kitano@ci.ritsumei.ac.jp

Abstract. Brain functions such as learning and memory rely on synaptic plasticity. Many studies have shown that synaptic plasticity can be driven by the timings between pre- and postsynaptic spikes, also known as spike-timing-dependent plasticity (STDP). In most of the modeling studies exploring STDP functions, presynaptic spikes have been postulated to be Poisson (random) spikes and postsynaptic neurons have been described using an integrate-and-fire model, for simplicity. However, experimental data suggest this is not necessarily true. In this study, we investigated how STDP worked in synaptic competition if more neurophysiologically realistic properties for pre- and postsynaptic dynamics were incorporated; presynaptic (input) spikes obeyed a gamma process and the postsynaptic neuron was a multi-timescale adaptive threshold model. Our results showed that STDP strengthened specific combinations of pre- and postsynaptic properties; regular spiking neurons favored regular input spikes whereas random spiking neurons did random ones, suggesting neural information coding utilizes both the properties.

Keywords: Synaptic plasticity, synaptic competition, interspike intervals, adaptive spike threshold.

1 Introduction

Synaptic plasticity is a physical change in synapses that embeds learning and memories in neural circuits. A significant neural activity encoding such a cognitive function is transformed into a configuration of synaptic strengths, suggesting that the activity patterns strengthening synapses should be the method by which neural information is coded. Many experimental studies have reported that synapses undergo changes depending on the relative timings between pre- and postsynaptic spikes, which is called spike-timing-dependent plasticity (STDP) [1, 2]. To understand the functional roles of STDP, many computational models have been proposed thus far [3, 4]. According to those studies, STDP regulates the firing rate of postsynaptic neurons, bringing about competition between synapses, and detecting coherent neural activities. Most of those studies, however, have hypothesised that input spikes mediated by STDP synapses were Poisson (random) spikes and that the spike generation mechanism is well described

S. Wermter et al. (Eds.): ICANN 2014, LNCS 8681, pp. 733–740, 2014.

by the simple leaky integrate-and-fire (LIF) model. However, experimental and theoretical studies have shown that these hypotheses do not necessarily explain the mechanism [5–8]. Considering the significance of pre- and postsynaptic spike timings in STDP, an important issue is to investigate its functional roles in the case of more realistic temporal structures of synaptic inputs and spike generation mechanisms.

To address this issue, we incorporated more neurophysiologically realistic features into a computational model for synaptic competition by STDP [3]. In our model, interspike intervals (ISIs) of presynaptic spikes obey gamma distributions with various values of shape parameter. This implementation enables us to generate a wide spectrum of spike trains, from Poisson to periodic by changing the shape parameter. In addition, we adapted a multi-timescale adaptive threshold (MAT) model, not merely an LIF model, as the postsynaptic neuron because the MAT model is capable of mimicking the spiking activity of a real cortical neuron much more precisely than any other neuron model [9]. We investigated how the interplay between the pre- and postsynaptic features affects synaptic competition through STDP and what the most effective combination of these features to strengthen synapses is, which could act as the method of encoding for various cognitive functions.

2 Methods

In our model, a single postsynaptic neuron received synaptic inputs from 1,000 excitatory synapses and 200 inhibitory ones. We here focused on synaptic competition among only excitatory synapses and therefore fixed strengths (conductances) of the inhibitory synapses and the firing rate of inhibitory inputs.

2.1 Postsynaptic Neuron Model

The dynamics of the postsynaptic neuron was modeled by the MAT model [9] that was proven to most precisely reproduce the spiking activity of a cortical neuron. The membrane potential V of the MAT model obeyed the following linear differential equation:

$$\tau_{\mathrm{m}} \frac{dV}{dt} = -(V - E_{\mathrm{rest}}) + I_{\mathrm{syn}}, \tag{1}$$

where τ_{m} and E_{rest} are the membrane time constant and the resting membrane potential, respectively. I_{syn} is the sum of synaptic currents mentioned below. When the membrane potential V reached the time-varying threshold $\theta(t)$, the neuron is supposed to emit a neuronal spike without the resetting used in an LIF model. The time course of $\theta(t)$ was described by

$$\theta(t) = \theta_{\infty} + \sum_{t_i^{\mathrm{spk}} < t} \left(\alpha_1 e^{-(t - t_i^{\mathrm{spk}})/\tau_1} + \alpha_2 e^{-(t - t_i^{\mathrm{spk}})/\tau_2} \right), \tag{2}$$

where θ_∞, α_n and τ_n ($\tau_1 < \tau_2$) are the constant component, amplitudes of time-varying components, and the time constant, respectively. Each time-varying component of $\theta(t)$ increased instantaneously at every spike timing t_i^{spk} by α_n and then exponentially decayed. As the MAT neuron evoked spikes faster than the time-varying components decayed, the adaptive spike threshold was gradually increased and then its neuronal spiking slowed down. In particular, the time-varying component with the time constant of 100 to 200 ms was responsible for this spike frequency adaptation seen in a 'regular-spiking' neuron, the majority of excitatory cortical neurons.

2.2 Synaptic Currents

The synaptic inputs consisted of both excitatory and inhibitory inputs

$$I_{\mathrm{syn}} = \sum_{j=1}^{1000} g_j^{\mathrm{ex}}(E_{\mathrm{ex}} - V) + \sum_{k=1}^{200} g_k^{\mathrm{in}}(E_{\mathrm{in}} - V), \tag{3}$$

where g_j^{ex}, g_k^{in}, E_{ex} and E_{in} are the conductance of the j-th excitatory synapse, the conductance of the k-th inhibitory synapse, the reversal potential of excitatory synapses, and reversal potential of inhibitory synapses, respectively. Changes in g_j^{ex} and g_k^{in} obeyed the simple first-order kinetics; they instantaneously increased at a presynaptic spike timing and then decayed exponentially. The peak conductance of g_j^{ex} engaged in the spike-timing-dependent plasticity defined by pre- and postsynaptic spike pairs and the additive rule [3].

2.3 Presynaptic Spike Trains

The $(i+1)$-th spike timing t_{i+1} is generated by adding an ISI, T_i, to the previous timing t_i, namely, $t_{i+1} = t_i + T_i$. The ISI T_i was drawn from the gamma distribution

$$T_i \sim p(t; k, \lambda) = \frac{\lambda^k t^{k-1} e^{-\lambda t}}{\Gamma(k)}, \tag{4}$$

where k, λ and $\Gamma(k)$ are a shape parameter, a rate parameter, and a gamma function, respectively. The mean of ISIs, $\bar{T}$, is $\bar{T} = \frac{k}{\lambda}$. The shape parameter k defines the shape of the distribution. If $k = 1$, the $p(t; 1, \lambda)$ is equivalent to the exponential distribution with a rate parameter λ. For a larger k, the distribution takes a symmetric shape, like a normal distribution, and consequently such a spike train exhibits nearly periodic firing. A spike train was generated by the ISI distribution independently of other spike trains.

2.4 Numerical Simulations

In order to examine how synaptic competition is affected by the interplay between the features of input spikes and postsynaptic dynamics, we compared

different combinations of the pre- and postsynaptic features. Typically, the input spikes were generated by the gamma distribution with $k = 1$ or with $k = 2$ whereas the LIF or the MAT model were implemented as the postsynaptic neuron. In the last investigation, 1,000 excitatory synapses were divided into 10 subgroups (100 synapses per a subgroup). Synapses in a subgroup delivered spike trains generated by the gamma distribution with an identical shape parameter; the parameter for the i-th group was set to $k = i$.

The parameters of the MAT model were: $\tau_{\mathrm{m}} = 20\mathrm{ms}$, $\theta_{\infty} = -58\mathrm{mV}$, $\tau_1 = 20\mathrm{ms}$, $\tau_2 = 200\mathrm{ms}$, $\alpha_1 = 20\mathrm{mV}$, and $\alpha_2 = 3\mathrm{mV}$. The other parameters were the same as those in a previous study [3].

3 Results

For various input firing rates, we conducted numerical simulations using our computational model until the distribution of synaptic strengths reached a stationary state. We here focused on this stationary distribution of synaptic strengths and the firing characteristics of the postsynaptic neuron in the stationary state.

3.1 Dependence on Postsynaptic Dynamics

First, we examined the synaptic competition mediated by the MAT model. Figure 1 shows the stationary distributions of synaptic strengths for various input firing rates and the spike statistics of the postsynaptic neuron in the stationary state. As shown in Fig. 1a–d, all the distributions exhibited bimodal shapes in which there existed a population of strengthened synapses (around 1) and that of weakened synapses (around 0). As the input firing rate was increased, the population of strengthened synapses became smaller, whereas that of the weakened ones became larger. Fig. 1e indicates that the postsynaptic firing rate was smaller than the case of an LIF model (10–15Hz) and that coefficients of variation (Cv) of postsynaptic ISIs were also much smaller than the previous ones (~ 0.9) [3]. The obtained spike statistics looked different from those of an LIF model, which can be attributed to the spike generation mechanism of the MAT model. However, we found that synapses competed with each other in a manner similar to that found in a previous study [3].

3.2 Dependence on Temporal Structures of Input Spike Trains

Next, to see how synaptic competition was affected by spike trains obeying a gamma process, such spike trains were fed into the LIF and MAT neuron models. Spike trains were generated by the gamma distribution with $k = 2$. The rate parameter was adjusted so that the means of ISIs were kept to the inverse of a preset input firing rate. Moreover, in this case, stationary distributions of synaptic strengths exhibited bimodal shapes similar to Fig. 1a–d (not shown). As shown in Fig. 2a and b, the firing rates of both models saturated with an increase in the input firing rate. The Cv of the LIF neuron decreased in comparison with

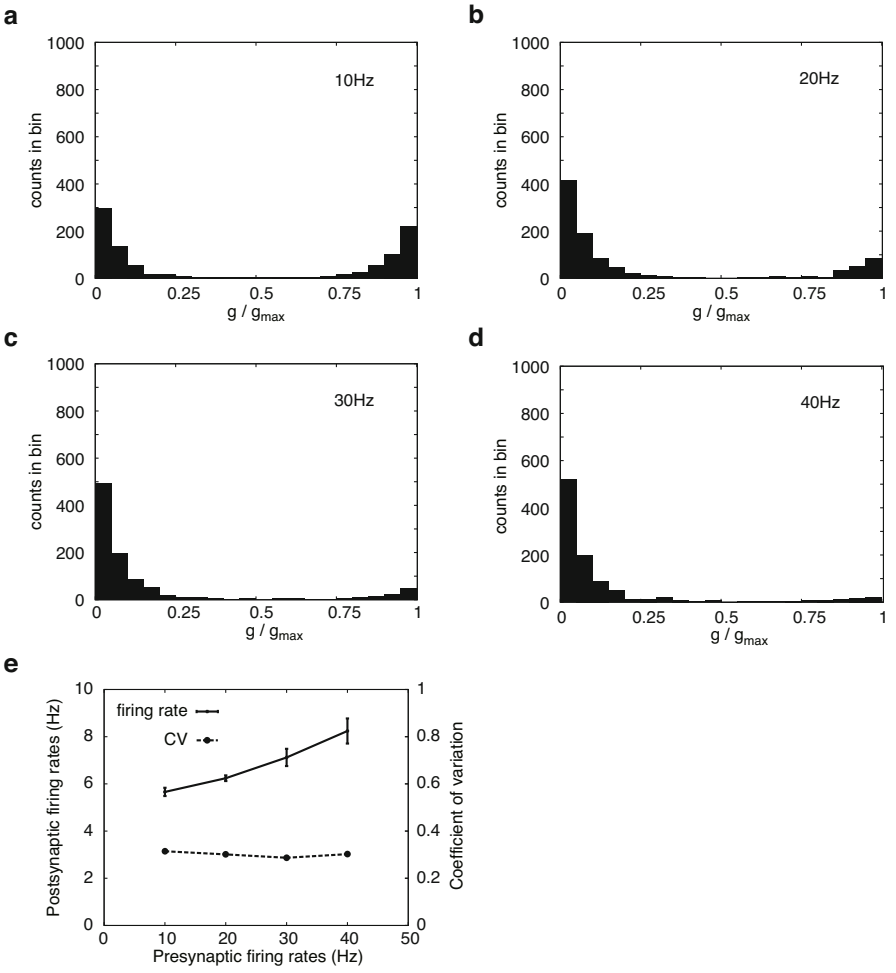

Fig. 1. Synaptic competition and activity regulation when the MAT model received Poisson spike trains ($k = 1$). **a.** Stationary distributions of synaptic strengths for the input firing rate of 10 spikes/s. The abscissa axis indicates the normalised synaptic conductance. **b**, **c**, and **d** are similar to **a**, but for 20 spikes/s, 30 spikes/s and 40 spikes/s, respectively. **e.** Dependencies of postsynaptic firing rates and coefficients of variation (Cv) on input firing rates.

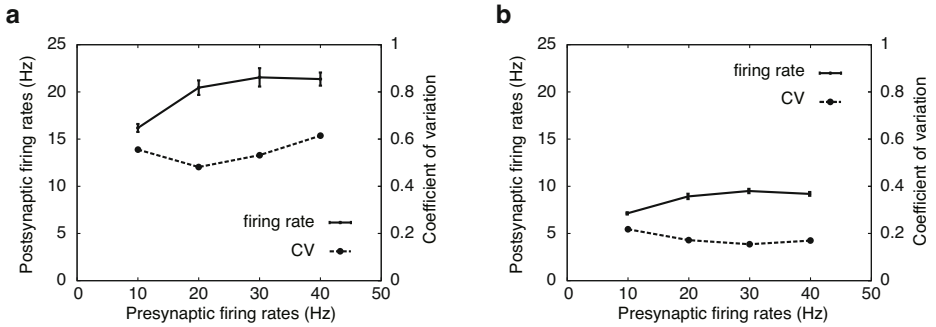

Fig. 2. Activity regulation for input spike trains obeying the gamma process. **a.** Dependencies of the postsynaptic firing rates and Cv on the input firing rates when the LIF model received spike trains generated by the gamma distribution with $k = 2$. **b.** Similar to **a**, but in the case that the postsynaptic neuron is the MAT model.

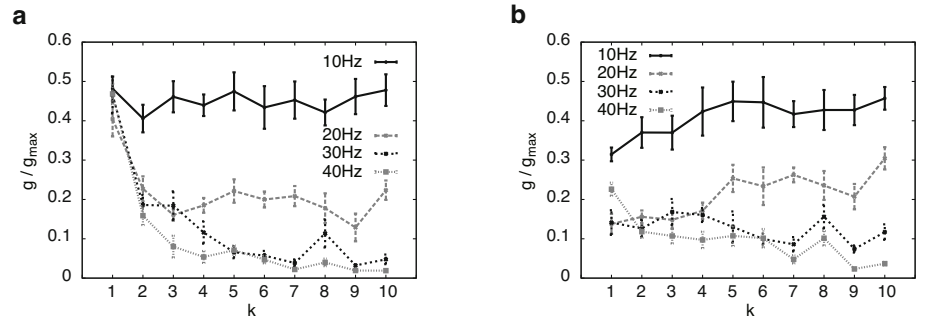

Fig. 3. Synaptic competition between synapses delivering spike trains with different ISI distributions. The abscissa axis represents a subgroup index, which corresponds to a value of the shape parameter for the subgroup. The ordinate axis indicates an averaged strength of synapses within a subgroup. The symbols and the error bars are the means and standard deviations of the averaged strengths for 10 trials. The cases of different input firing rates were examined, but the input firing rate was identical to all the synapses in a trial. **a.** and **b.** illustrate the case for an LIF model and for the MAT model, respectively.

that in the case of Poisson spike trains (~ 0.9) [3]. Similarly, the Cv of the MAT model became smaller than that shown in Fig. 1e. Irrespective of neuron models, spike trains could alter the spike statistics of the postsynaptic neuron, but not its synaptic competition.

3.3 Extracted Combinations of Pre- and Postsynaptic Features

Finally, we investigated whether each of the neuron models showed a preferred or favourite type of spike trains. In this simulation, the postsynaptic neuron

(LIF or MAT) received different types of spike trains from different subgroups of synapses; synapses in the i-th subgroup fed spikes generated by the gamma distribution with $k = i$ into the postsynaptic neuron. Figure 3 shows the synaptic strengths averaged over synapses in each subgroup for various input firing rates. For the LIF model (Fig. 3a), synapse strength in all the subgroups changed equally when the input firing rate was 10 Hz. In the case of higher input firing rates (20–40Hz), however, subgroups with the larger ks tended to be depressed, compared with the subgroup of $k = 1$. In contrast, the tendency was quite different for the MAT model (Fig. 3b). For the lower input firing rates (10 and 20Hz), synapses in subgroups with larger ks were strengthened. However, for the larger input firing rate (40Hz), those subgroups were more depressed. Thus, we found that the favoured spike trains depended on the neuron models and the input firing rates.

4 Discussion

Most of previous computational studies have assumed that spikes were randomly generated so that ISIs obeyed an exponential distribution. However, ISI distributions of experimentally recorded spike trains exhibit asymmetric unimodal shapes like Gamma distributions rather than exponential distributions. As for a computational neuron model, although an LIF model has been frequently used for simplicity, the model does not reproduce spiking activity of a real cortical neuron, for example, a regular spiking neuron that show spike frequency adaptation. These properties would have a considerable impact on many aspects of neuronal dynamics including activity-dependent neural network formation. Therefore, we studied synaptic competition brought about by STDP when we incorporated the more realistic properties of pre- and postsynaptic dynamics.

According to our results, as long as all synapses delivered spike trains with an identical feature (an ISI distribution), synapses competed similarly to how they did in a previous study [3] and stationary distributions of synaptic strengths were bimodal, irrespective of the choice of postsynaptic neuron model, or ISI distributions of input spikes. The bimodal shape emerged from the nature of the pairwise additive STDP rule that makes an unstable point at an intermediate strength [10], whereas the spike statistics of the postsynaptic neurons were influenced by the neuronal dynamics and the input ISI structures. For the case of a mixture of differently structured spike trains (with different k), strengthened synapses relied on combinations of the postsynaptic neuron models and the input ISI structures. Considering that spike trains mediated by strengthened synapses evoked postsynaptic spikes more effectively, we could determine which types of spike trains were favoured by the postsynaptic neuron by observing which synapses were strengthened. The LIF neuron favoured random spike trains for any input firing rate. In contrast, the MAT neuron favoured more regular spike trains (with a large k) for a lower input firing rate, but more random spike trains (with a small k) for a higher input firing rate. Taken together, the method of neural information encoding, by a configuration of synaptic strengths,

is determined not only by presynaptic spike structures but also by postsynaptic neuronal dynamics.

Previous studies have revealed that cortical neurons can be classified into several neuron types from the viewpoints of the shapes of their ISI distributions, and that the neuron-type distributions differ between cortical areas [5]. For example, in motor-related areas, neurons exhibiting regular spike trains were dominant over those exhibiting random spike trains, but the opposite was observed in the prefrontal areas. From our results, the MAT model, which exhibited low Cv spiking, favoured regular spike trains whereas the LIF, which exhibited high Cv spiking, favoured random spike trains. This suggests that our results are consistent with the previous analysis reported in [5]. Furthermore, this implies that different functions processed in different cortical areas should utilise different methods of neural information coding.

Here we assumed a stationary process for input spike trains, which might limit the biological plausibility of our results, for example, the obtained Cv values (Fig.2b) were much smaller than those of experimental spike data. Implementing non-stationary inputs would improve them. Furthermore, if a cognitive function is represented by a transient neural activity, it is necessary to take into account such non-stationary dynamics. Even in that case, however, our results would serve as the basis for related future studies.

References

1. Markram, H., Lubke, J., Frotscher, M., Sakmann, B.: Regulation of Synaptic Efficacy by Coincidence of Postsynaptic APs and EPSPs. Science 275, 213–215 (1997)
2. Bi, G.-Q., Poo, M.-M.: Synaptic Modifications in Cultured Hippocampal Neurons: Dependence on Spike Timing, Synaptic Strength, and Postsynaptic Cell Type. J. Neurosci. 18, 10464–10472 (1998)
3. Song, S., Miller, K.D., Abbott, L.F.: Competitive Hebbian Learning Through Spike-Timing-Dependent Synaptic Plasticity. Nat. Neurosci. 3, 919–926 (2000)
4. Izhikevich, E.M., Gally, J.A., Edelman, G.M.: Spike-Timing Dynamics of Neuronal Groups. Cereb. Cortex. 14, 933–944 (2004)
5. Shinomoto, S., Miyazaki, Y., Tamura, H., Fujita, I.: Regional and Laminar Differences in In Vivo Firing Patterns of Primate Cortical Neurons. J. Neurophysiol. 94, 567–575 (2005)
6. Shinomoto, S., Miura, K., Koyama, S.: A Measure of Local Variation of Inter-spike Intervals. Biosystems 79, 67–72 (2005)
7. Brette, R., Gerstner, W.: Adaptive Exponential Integrate-and-Fire Model as an Effective Description of Neuronal Activity. J. Neurophysiol. 94, 3637–3642 (2005)
8. Izhikevich, E.M.: Which Model to Use for Cortical Spiking Neurons? IEEE Trans. Neural Netw. 15, 1063–1070 (2004)
9. Kobayashi, R., Tsubo, Y., Shinomoto, S.: Made-to-order Spiking Neuron Model Equipped with a Multi-Timescale Adaptive Threshold. Front. Comput. Neurosci. 3, 9 (2009)
10. Cateau, H., Fukai, T.: A Stochastic Method to Predict the Consequence of Arbitrary Forms of Spike-Timing-Dependent Plasticity. Neural Comput. 15, 597–620 (2003)